

Exploring cell compatibility of a fibronectin-functionalized physically crosslinked poly(vinyl alcohol) hydrogel

Leonardo E. Millon,^{1,2} Donna T. Padavan,³ Amanda M. Hamilton,⁴ Derek R. Boughner,⁵ Wankei Wan^{1,3}

¹Axcelon Biopolymers Corporation, London, Ontario N6A 5B9, Canada

²Department of Chemical and Biochemical Engineering, The University of Western Ontario, London, Ontario N6A 5B9, Canada

³Biomedical Engineering Graduate Program, The University of Western Ontario, London, Ontario N6A 5B9, Canada

⁴Department of Anatomy and Cell Biology, The University of Western Ontario, London, Ontario N6A 5B9, Canada

⁵London Health Science Centre, The University of Western Ontario, London, Ontario N6A 5B9, Canada

Received 29 March 2010; revised 24 February 2011; accepted 9 March 2011

Published online 13 October 2011 in Wiley Online Library (wileyonlinelibrary.com). DOI: 10.1002/jbm.b.31860

Abstract: Physically crosslinked poly(vinyl alcohol) (PVA) hydrogels prepared using a low-temperature thermally cycled process have tunable mechanical properties that fall within the range of soft tissues, including cardiovascular tissue. An approach to render it hemocompatible is by endothelialization, but its hydrophilic nature is not conducive to cell adhesion and spreading. We investigated the functionalization reaction of this class of PVA hydrogel with fibronectin (FN) for adhesion and spreading of primary porcine radial artery cells and vascular endothelial cells. These are cells relevant to small-diameter vascular graft development. FN functionalization was achieved using a multistep reaction, but the activation step involving carbonyl diimidazole normally required for

chemically crosslinked PVA was found to be unnecessary. The reaction resulted in an increase in the elastic modulus of the PVA hydrogel but is still well within the range of cardiovascular tissue. Confocal microscopy confirmed the adhesion and spreading of both cell types on the PVA–FN surfaces, whereas cells failed to adhere to the PVA control. This is a first step toward an alternative for the realization of a synthetic replacement small-diameter vascular graft. © 2011 Wiley Periodicals, Inc. *J Biomed Mater Res Part B: Appl Biomater* 100B: 1–10, 2012.

Key Words: poly(vinyl alcohol), hydrogel, fibronectin, functionalization, cell compatibility

How to cite this article: Millon LE, Padavan DT, Hamilton AM, Boughner DR, Wan W. 2012. Exploring cell compatibility of a fibronectin-functionalized physically crosslinked poly(vinyl alcohol) hydrogel. *J Biomed Mater Res Part B* 2012;100B:1–10.

INTRODUCTION

The most common vascular graft replacements for coronary artery bypass surgery (CABG) are the patient's saphenous vein, internal thoracic artery, and radial artery from the arm. These autologous bypasses are problematic in that they deteriorate over time because of further advancement of the patient's atherosclerotic disease, they disrupt the normal vascularity, and autologous sources may not provide sufficient native vessels for multiple bypass surgery.¹ The most popular polymer-based synthetic vascular prostheses are those derived from polyethylene terephthalate (PET) and expanded polytetrafluoroethylene (ePTFE). These grafts perform well as large-diameter (>6 mm) peripheral grafts under high-flow and low-resistance conditions but are not suitable for small-diameter (<5 mm) arterial reconstructions such as CABG because they are prone to induce thrombus and stenosis. Another important consideration is the mismatch in mechanical properties between the graft material and native tissue at the suturing junction. It is

believed that this plays a major role in postoperative complications and ultimate failure.^{2,3}

Graft passivation is a method of improving the patency of these synthetic grafts by surface modification with proteins, polymeric materials, and cells to minimize material–blood interactions. The most common methods investigated include treating the polymer with biological agents such as heparin, prostaglandins, growth factors, and anticoagulant peptide sequences.⁴ Another approach is endothelialization of the inner surface of the conduit to provide a nonthrombogenic living lining to interface with blood. Most of the research in this area is focused on modifying the surface with extracellular matrix proteins (fibronectin [FN], laminin) or adhesive amino acid sequences Arg-Gly-Asp (RGD) to promote endothelial cell (EC) attachment and migration. After modification, autologous ECs are seeded onto the luminal surface of the graft to allow the formation of a confluent monolayer of ECs before implantation. Even though the surface-modified grafts of PET and ePTFE have improved cell adhesion, their

Correspondence to: W. Wan; e-mail: wkwan@eng.uwo.ca

mismatch of mechanical properties still hinders their long-term performance as a small-diameter bypass graft.^{2,5-7}

From a structural point of view, cardiovascular tissues are composed mainly of elastin and collagen, with elastin providing the elasticity and collagen providing the strength. Thus, its overall mechanical behavior is nonlinear. It is also viscoelastic and anisotropic in nature.^{8,9} Poly(vinyl alcohol) (PVA) is a well-known biomaterial that has been investigated for various biomedical applications.¹⁰⁻¹³ Of particular relevance is PVA, which has controlled mechanical properties and is formed by physically crosslinking PVA using a low-temperature thermal cycling process. The mechanical characteristics of such PVA hydrogels are similar to that of soft tissue, including nonlinear stress-strain relationships, elasticity, and strength, and can be controlled by changing the PVA solution concentration and thermal processing parameters.^{10,11,14,15} Furthermore, creation of the desired amount of anisotropy in PVA and PVA-bacterial cellulose hydrogels that mimics the mechanical properties of porcine aorta in both circumferential and axial directions has also been reported.¹⁶⁻¹⁹

Functionalization of PVA with FN to promote cell adhesion has been reported.²⁰⁻²³ It generally involves three chemical reactions, namely, the linkage of a long alkyl chain containing an acid group to the —OH groups of PVA followed by activation of the acid group toward nucleophilic attack with carbonyl diimidazole (CDI). The final step is the reaction of the PVA-CDI derivative with FN. The PVA used in these FN functionalization reactions have all been chemically cross-linked via the —OH groups attached to its carbon backbone.

This article describes the design and development of a PVA hydrogel-tissue hybrid material. A physically cross-linked PVA hydrogel made by the low-temperature thermal cycling technique was chemically functionalized with FN, a well-known adhesive protein. This functionalized PVA hydrogel was evaluated for its mechanical properties and compared with that of porcine aorta. Porcine ECs and radial artery cells (RACs) were also seeded independently onto the FN-functionalized PVA hydrogel to assess their cell compatibility and relevance to small-diameter conduit development.

MATERIALS AND METHODS

PVA solution preparation

PVA (Sigma-Aldrich Co.) with a molecular weight (M_w) of 146,000–186,000, 99+ % hydrolyzed, was used in all solution preparations. PVA was added to distilled water to obtain a 10 wt % PVA solution. This mixture was heated for 3 hr at 90°C using a setup previously reported.^{16-19,24}

Samples preparation

Mechanical and cell seeding sample preparation. A 10% PVA solution was transferred into an aluminum mold with a 1.5-mm gasket and placed in the heated/refrigerated circulator, where they were cycled six times between 20°C and –20°C to give cycle six samples, which have previously shown to give a stable hydrogel.¹⁶⁻¹⁹ All samples, both reacted and controls, were initially cut ($25 \times 5 \text{ mm}^2$) for tensile testing ($n = 5$). The PVA-FN reaction (with and without CDI step) samples were allowed to fully reswell in phosphate-buffered saline (PBS) for 3 weeks before tensile testing.

For cell seeding samples, 10% PVA solution was transferred into a custom made aluminum mold specifically designed to make samples of $\sim 150 \mu\text{m}$ in thickness. This mold was required because 1.5-mm-thick opaque PVA samples (for mechanical testing) were too thick for visualization using confocal microscopy after cell seeding. These samples were cycled as described above. All samples, reacted and controls, were initially cut in the shape of discs using an 11-mm diameter custom-designed punch for cell seeding purposes ($n = 2$ for each condition). The cell seeding on PVA controls and reacted PVA samples was performed in three independent trials to verify reproducibility (i.e., total $n = 6$ for each condition).

PVA functionalization with FN

FN functionalization of PVA hydrogels was accomplished by adapting a procedure previously reported for glutaraldehyde crosslinked PVA samples.²⁰ The sequence of reactions are shown as PATH 2, $1+2 \rightarrow 3 \rightarrow 4 \rightarrow 5$ in Figure 1, which corresponds to PVA functionalized with FN via CDI (Sigma-Aldrich Co.). The procedure first required the linkage of a long alkyl chain **2** containing an acid group to hydroxyl groups of **1**. Several PVA hydrogel disks (**1**) were added to 20 mL of cold 3M NaOH in a reaction flask. Approximately 200 mg of **2** (Sigma-Aldrich Co.) was added to the reaction flask, while heating to 37°C and mixing at 250 rpm for 4 hr. The disks from each flask were rinsed with distilled H₂O several times to remove impurities forming intermediate **3**. Samples were then allowed to dry overnight in a vacuum oven. The next step involved activating the acid group in **3** toward nucleophilic attack with CDI. For this step, dried PVA disks (intermediate **3**) were added to 20 mL of acetone and 500 mg of CDI in the reaction flasks and allowed to react for 4 hr at room temperature and 250 rpm. The dried disks were then rinsed thoroughly with acetone, forming intermediate **4**. For the final reaction, the PVA disks (intermediate **4**) were sterilized under UV light for 1 hr in a sterile hood. A solution of 0.1M sodium carbonate buffer (pH 9–10) was prepared and sterilized using a 0.45- μm filter. Approximately 1 mg of FN from bovine plasma (FN; Sigma-Aldrich Co.) was added to 20 mL of the sodium carbonate buffer, and the disks (intermediate **4**) were allowed to react for 4 hr at room temperature and 250 rpm. Samples were rinsed with PBS, forming product **5**, and then placed in their respective media (for ECs or RACs) overnight to remove any unreacted FN.

FN functionalization of PVA hydrogels without CDI (PATH 1) was also performed (Figure 1). The reaction conditions to form intermediate **3** were the same as described above for PATH 2. Similarly, the reaction conditions between **3** and **5** are the similar to the reaction conditions between **4** and **5** previously discussed.

Four different groups of samples were tested for FN covalent bonding (immunostaining) and cell seeding. The groups were PVA control (as made), PVA soaked in FN solution (no reaction), PVA-FN without CDI step (PATH 1), and PVA-FN with CDI step (PATH 2). PATH 1 was used as a negative control in the literature,²⁰ but we wanted to test all

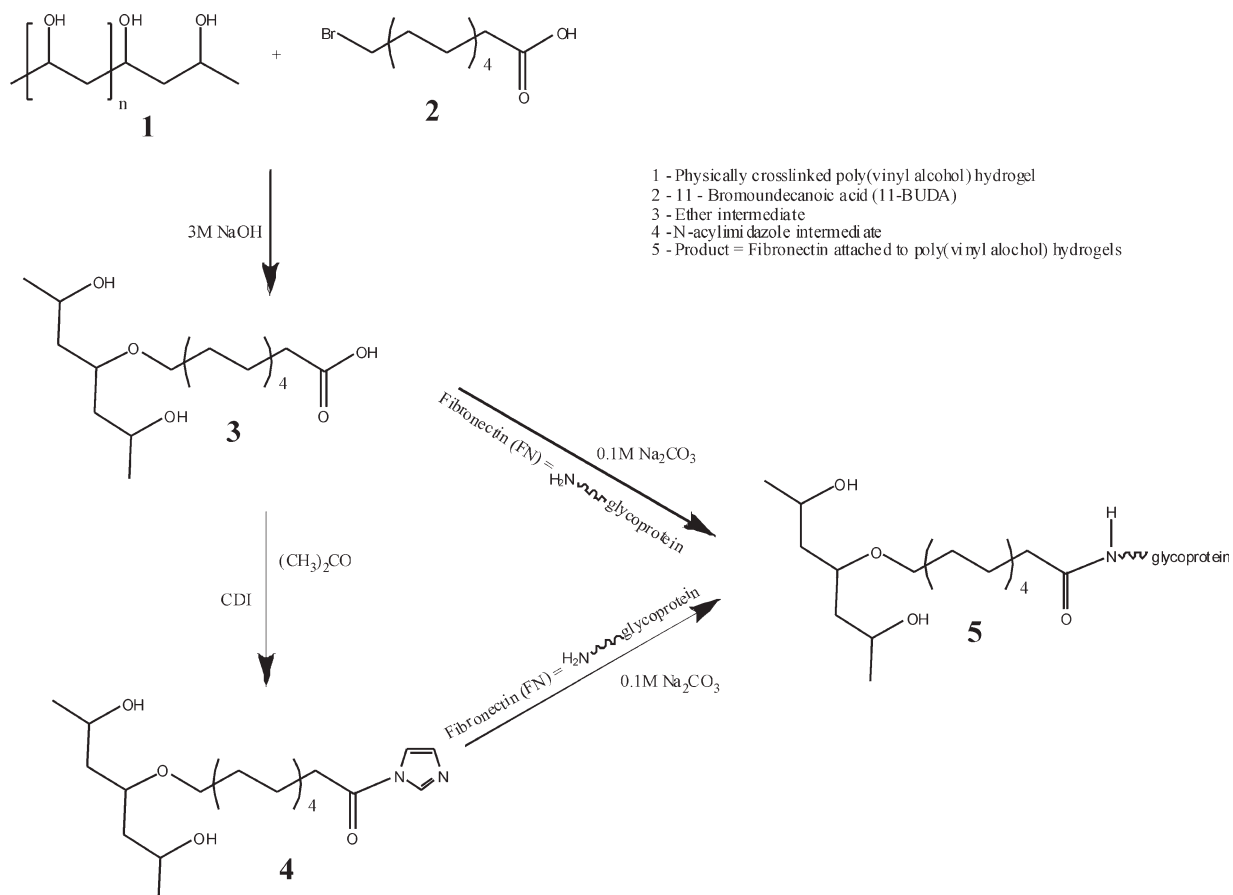


FIGURE 1. Schematic of poly(vinyl alcohol) hydrogels functionalized via fibronectin by two pathways: PATH 1, without CDI (1+2 → 3 → 5); PATH 2, with CDI (1+2 → 3 → 4 → 5).

possible scenarios for comparison purposes. Fourier transform infrared (FTIR) characterization of PVA, PATH 1, and PATH 2 was also investigated.

Mechanical testing

Tensile testing. The testing equipment consists of a servo-hydraulic material testing system (INSTRON 8872) equipped with a 1-kg load cell, as described previously.^{16–19} Sample thickness was measured, and testing was performed inside a Plexiglas tank filled with PBS kept at 37°C. All the specimens were secured onto custom-designed tissue grips with a ~10-mm grip-to-grip distance, and tensile tests were performed at a crosshead speed of 40 mm/s to a maximum of 65% strain. Before the tensile tests, all specimens were preconditioned with 10 loading and unloading cycles, as previously reported.^{16–19}

The data obtained was in the form of load extension, which was then converted into engineering stress-engineering strain, using the sample thickness and the initial gauge length after preconditioning. The stress-strain data for all PVA hydrogels (controls and reacted) are nonlinear and take on the general shape of curving up toward the stress axis. Therefore, the stress-strain data were fitted by a three-parameter exponential growth equation. The elastic modu-

lus, at a particular strain, can be calculated by the first derivative of this equation, as reported previously.^{16–19,24}

Stress-strain data were obtained up to 65% strain, which was still within the elastic region for the tested PVA-based hydrogels and covers the cardiovascular physiologic strain range. For cardiovascular applications, it is important to design a material that is able to remain elastic at higher strains than normal physiologic values (~20–30%) for cases corresponding to higher systolic pressures.^{14,16–19,25}

Stress relaxation testing. The time-dependent properties of all samples were assessed by a stress relaxation test. After preconditioning and tensile testing, some samples ($n = 3$) were strained to the same 65% strain used for tensile testing and held at constant strain for 1 hr, while monitoring the load.

The raw data were collected in the form of load time and converted to relative stress remaining time, relative to the initial stress at time zero. The stress relaxation data were fitted to a five-parameter exponential decay equation, as described previously.^{16,18,19}

Statistical analysis

For statistical comparisons, a one-way analysis of variance was performed, as described previously.^{16–19,24}

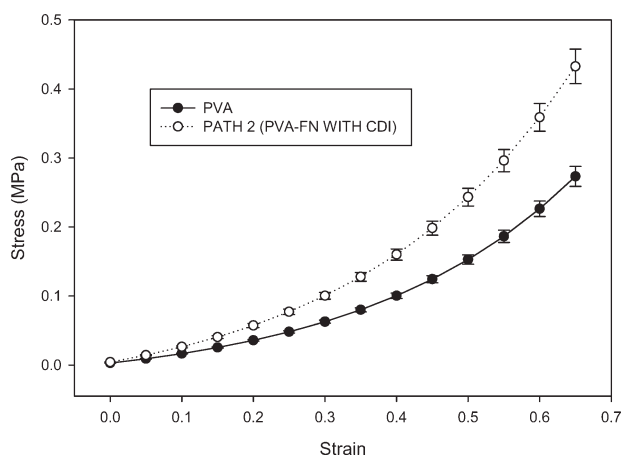


FIGURE 2. Stress–strain response of the PVA control and PATH 2 (PVA–FN with CDI) samples.

FTIR characterization

FTIR spectra were obtained from dehydrated samples of PVA control, PVA–FN (PATH 1), and PVA–FN (PATH 2) using a Bruker Vector 22 FTIR spectrometer (Milton, ON) equipped with an IR Scope 2 microscope at a crystal angle of 45°. The spectra were collected with a resolution of 4 cm^{-1} in absorption mode. Typically, 100 scans were averaged to reduce spectral noise. The spectra were baseline corrected using OPUS-NT 3.1 software.

Immunostaining testing for FN covalent attachment

Immunostaining was used to test for the covalent attachment of FN, as described previously.²⁰ The four different groups of samples described before were tested for FN attachment. As noticed, FN-soaked samples were tested as made and after soaking in media or PBS for up to 24 hr to imitate the effect of cell culturing on the samples and clarify the cell seeding results. In summary, all samples (reacted and unreacted) were incubated at 37°C for 15 min with 250 μL of goat blocking serum [1% (w/v) bovine serum albumin (BSA, Sigma-Aldrich Co.), 5% (v/v) goat serum (Sigma-Aldrich Co.)]. A mouse monoclonal anti-FN antibody (clone IST-3, Sigma-Aldrich Co.) was diluted 1:100 in 1% (w/v) BSA, and 50 μL /sample was added and placed in the incubator at 37°C for 1 hr. Samples were then washed with PBS-T (1 \times PBS with 0.05% Triton-X100) three times for 5 min each. An Alexa Fluor® 488 goat anti-mouse IgG secondary antibody (Invitrogen, Canada) was diluted 1:1000 in 1% (w/v) BSA, added at 50 μL /sample, and placed in the incubator at 37°C for 1 hr. Samples were then washed with PBS-T three times for 5 min each. Finally, duplicate samples for each condition were mounted on coverslips with fluorescent mounting media (Dako, Canada) and allowed to dry at 4°C overnight. Confocal microscopy was performed on all samples to visualize FN, given that any immunofluorescence should convey covalent attachment of FN to the PVA surface. A Zeiss LSM 410 laser-scanning confocal microscope system and LSM-PC imaging software (Carl Zeiss Canada) was used to obtain all micrographs. Desorption of FN from reacted

samples (PATHS 1 and 2) using 70 % isopropanol before antibody staining was also implemented in duplicates, as described by Nuttelman et al.²⁰ Also note that serum-free media was used for the soaking stages that did not require cells to be present. Serum was present in the media at any point where cells were involved; 10% fetal bovine serum (FBS) for M199 and 5% of endothelial growth medium (EGM).

Cell seeding of FN-functionalized PVA

FN-functionalized PVA hydrogels are expected to promote both RACs and ECs attachment to the hydrogel surface. Both types of primary culture cells were harvested enzymatically and isolated from porcine tissues, as previously described.^{26,27} RACs were maintained in Medium 199 (M199) supplemented with 10% FBS (Invitrogen) and 1% penicillin/streptomycin (Invitrogen). Vascular ECs were maintained in EGM with 5% FBS, 1% penicillin/streptomycin and a bullet kit containing rhEGF, rhFGF-B, vascular endothelial growth factor, R³-IGF-1, gentamicin/amphotericin, hydrocortisone, and ascorbic acid (Lonza, Canada). All cells were kept in an incubator at 37°C (5% CO₂). Under sterile conditions, a suspension of RACs (passages 3–6) and ECs (passages 3–5) in their respective medium were seeded onto all types of PVA samples at high densities (250,000 cells/cm²) and allowed to adhere. Cell spreading was assessed using confocal microscopy in duplicates at 4, 8, and 24 hr. Cell seeding experiments were repeated three independent times. After cell seeding for the required amount of time, samples were fixed in 10% formalin for 1 hr at room temperature and stored in PBS at 4°C before immunolabeling.

RACs were stained with monoclonal mouse antismooth muscle α -actin–Cy3-conjugated IgG2a primary (clone 1A4, 1:50) (Chemicon, CA). ECs were incubated with polyclonal rabbit anti-human Von Willebrand factor primary IgG (A0082, 1:50) (Dako, Canada) and AlexaFluor® 488 goat anti-rabbit IgG secondary (1:200) (Invitrogen Molecular Probes, OR). Cell nuclei were labeled with Hoechst 33342. After immunolabeling, duplicates of each condition were mounted on coverslips with fluorescent mounting media (Dako, Canada). All immunolabeled samples were analyzed with confocal microscopy, as previously described. Phase contrast microscopy was initially implemented, as described by Nuttelman et al.,²⁰ but no clear view of cells was obtained because of the opaque nature of physically cross-linked PVA samples.

RESULTS

Effect of FN functionalization on tensile properties

Figure 2 shows the stress–strain response of the PVA control and PATH 2 (Figure 1). The FN-functionalized material is stiffer, but the nonlinear stress–strain relationship typical of soft tissues is retained. For comparison, at 65% strain, the PATH 2 samples display an elastic modulus of 1.60 ± 0.11 MPa, compared with a value of 1.02 ± 0.07 MPa for the PVA control, which corresponds to a 57% increase in stiffness. A similar stiffening effect was seen on the PATH 1

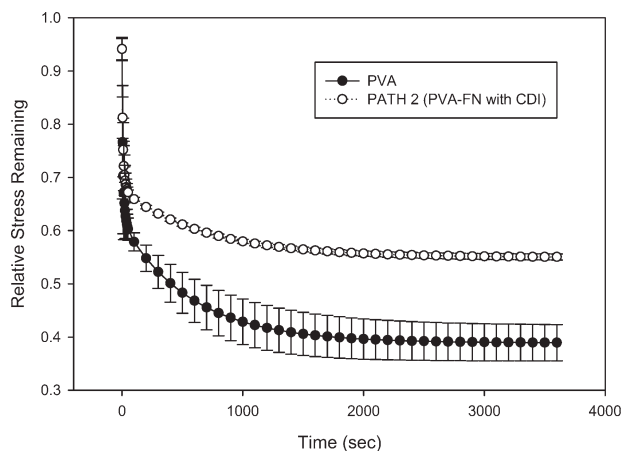


FIGURE 3. Stress relaxation response for the PVA control and PATH 2 (PVA-FN with CDI) samples.

samples (1.58 ± 0.09 MPa at 65% strain). The effect of testing in distilled H_2O versus PBS was also investigated using the PVA control samples. No difference in stiffness was observed. The data in Figure 2 show a statistically significant difference at 65% strain between the PATH 2 and the PVA control samples ($p < 0.05$).

Effect of FN functionalization on stress relaxation properties

The time-dependent relaxation response of the PVA control and the PVA-functionalized FN samples was assessed to determine the ability of the functionalized hydrogel to relax under tension. Figure 3 shows the stress relaxation response for the PVA control and PATH 2 samples. It is seen that the PVA control samples relax to a lower residual stress than the PATH 2 samples. The data in Figure 3 show a statistically significant difference of the residual stress at 1 hr for the PATH 2 and the PVA control samples ($p < 0.05$).

FTIR characterization of PVA-functionalized FN samples

FTIR was used to characterize the PVA hydrogel before functionalization with FN. In particular, it was used to identify the presence of functional groups characteristic of FN. The spectra of the PVA control, PATH 1, and PATH 2 samples are shown in Figure 4. As expected, in all samples, major peaks associated with PVA were observed. These include a broad stretching band between 3150 and 3550 cm^{-1} ($-OH$) and stretching bands at 2923 and 2842 cm^{-1} ($C-H$; asymmetric and symmetric). Another characteristic band for PVA was located between 1100 and 1200 cm^{-1} . The peak at approximately 1100 cm^{-1} ($C-O$) is indicative of the PVA's crystallinity.²⁸ Success of the functionalization reactions and the positive identification of FN comes from the presence of the amide I and amide II bands. The sharp peak at 1650 $cm^{-1,29,30}$ represents amide I ($C=O$ vibration), and a weak neighboring peak at 1580 $cm^{-1,30}$ is associated with amide II ($C-O$ stretching and $N-H$ bending), which are absent in the PVA control sample, thus confirming attachment of FN to the PVA hydrogel.

Immunostaining of PVA-FN

Immunostaining was used to confirm FN covalent attachment to the PVA backbone. Figure 5 shows the micrographs of PVA, PVA soaked in FN, PATH 1 samples, PATH 2 samples, and PVA soaked in FN samples followed by immersion in media (M199) for 4 and 24 hr. Indirect immunofluorescence of the attached FN was observed mainly in the reacted samples, PATH 1, and PATH 2 samples. Some fluorescence was initially observed in the PVA soaked in FN (physical absorption), but this fluorescence disappeared after soaking in either media or PBS (data not shown) for 4 and 24 hr. These results are consistent with the observations in the cell seeding results section. Desorption of FN from reacted samples (both PATH 1 and 2) using 70% isopropanol before antibody staining, but no difference in fluorescence was observed compared with non-isopropanol treated samples (data not shown).

Cell seeding of FN-functionalized PVA samples

Figure 6 shows the confocal micrographs of RACs seeded onto PVA control [Figure 6(A-C)], PVA soaked in FN [Figure 6(D-F)], PVA-FN samples prepared via reaction PATH 1 [Figure 6(G-I)] and PATH 2 [Figure 6(J-L)] for 4, 8, and 24 hr. RACs clearly adhere and spread well over both PVA-FN sample surfaces (PATH 1 and PATH 2), indicating that the CDI activation step may not be necessary. At all time points used (4, 8, and 24 hr), the PVA control and the PVA soaked in FN samples only showed a few randomly spaced rounded cells, indicating poor adherence and no cell spreading. Figure 7 shows the confocal micrographs of ECs

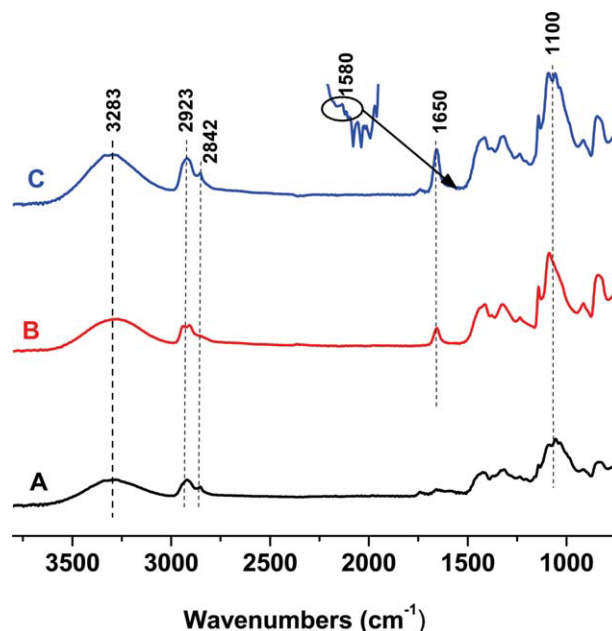


FIGURE 4. Fourier transform infrared spectra: (A) PVA control sample, (B) PATH 1 (without CDI) samples and (C) PATH 2 (with CDI) samples. All samples were washed three times with 60 mL of PBS. [Color figure can be viewed in the online issue, which is available at wileyonlinelibrary.com.]

Immunostaining of Fibronectin (FN)

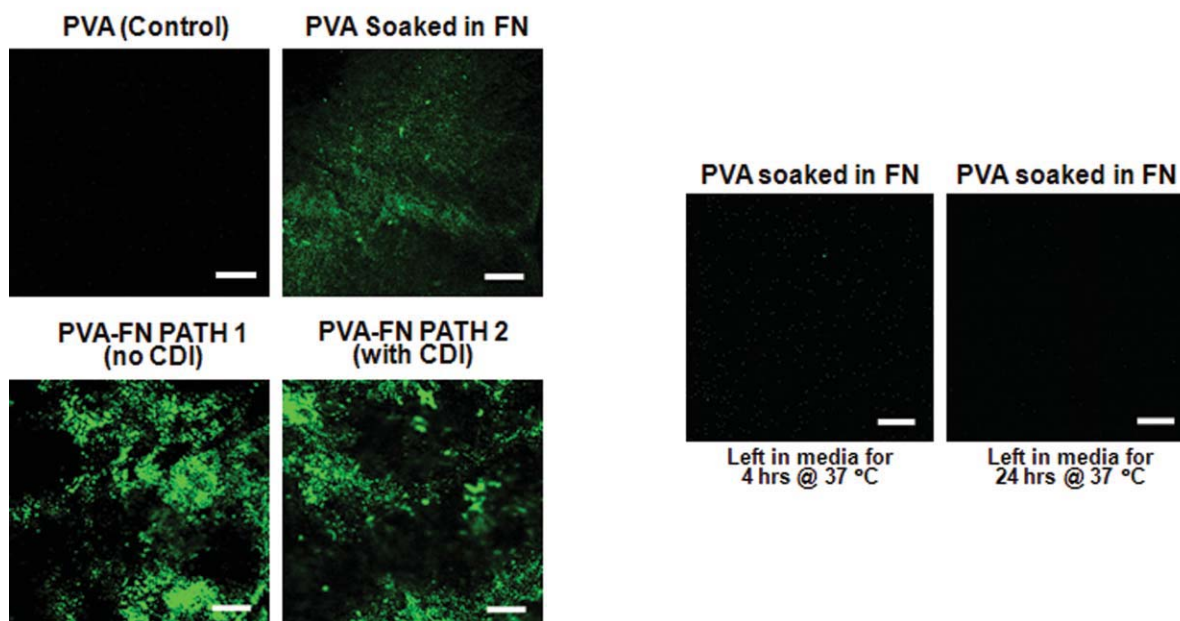


FIGURE 5. Confocal micrographs of PVA, PVA soaked in FN, PATH 1 (without CDI) samples, and PATH 2 (with CDI) samples, including results of soaking the PVA soaked in FN samples for 4 and 24 hr in media. Fifty-micrometer scale bar. Note: Serum free media was used for the soaking stages that did not require cells to be present. Serum was present in the media at any point where cells were involved; 10% FBS for M199 and 5% of EGM. [Color figure can be viewed in the online issue, which is available at wileyonlinelibrary.com.]

seeded onto PVA control [Figure 7(A–7C)], PVA soaked in FN [Figure 7(D–F)], PATH 1 [Figure 7(G–I)], and PATH 2 [Figure 7(J–L)] samples for 4, 8, and 24 hr. The results are similar to the RACs results in Figure 6, indicating the success of the FN functionalization reaction by both PATHS 1 and 2 and the necessity of FN for cell compatibility of the PVA hydrogel.

DISCUSSION

For a biomaterial to be useful for tissue replacement, it is important to ensure that it is both biocompatible and possesses mechanical properties similar to the surrounding host tissue.^{3,31} If the material is in direct contact with blood as in the case of vascular grafts, the added criteria of hemocompatibility has also to be satisfied. Of the currently approved synthetic graft materials such as Dacron and ePTFE, there is a large mechanical mismatch with the aortic tissue being replaced, which may contribute to intimal hyperplasia and ultimate failure.^{4,6}

In addition, these materials are not truly hemocompatible and as a result they can only be used for large-diameter replacements (>5 mm). A small-diameter (<5 mm) conduit made of synthetic biomaterial suitable for use in CABG is yet to be realized. As a first step toward the development of a biomaterial suitable for consideration for small-diameter vascular grafts, we investigated the use of a biomaterial that is tailored to have mechanical properties closely mimicking that of aortic tissue as the substrate and demonstrate endo-

thelization of its surface via functionalization with FN for attachment of ECs.

The substrate we chose to use was physically crosslinked PVA prepared by the freeze–thaw method¹⁴ as opposed to chemically crosslinked PVA. It consists of networks held together by molecular entanglements and/or secondary forces such as hydrogen bonding, Van der Waals interactions, and intramolecular hydrophilic associations, and it has a heterogeneous structure with phase-separated domains. In the initial freeze–thaw cycle, ice crystals in the amorphous regions force the polymer chains into regions of high local polymer concentration, forming crystallites. Further cycling increases the overall crystallinity by increasing the size of primary crystallites, as well as forming additional smaller secondary crystallites, transforming the microstructure into a fibrillar network. The crystallites have dimensions of about 3 nm and are separated by amorphous regions of approximately 20–30 nm in size within the polymer-rich regions. These polymer-rich regions are surrounded by polymer-poor regions (macropores) with dimensions of >100 nm.^{17,32,33} The porous structure arises from the existence of the polymer-poor regions, which are essentially filled with water.¹⁷ Chemically crosslinked hydrogels are covalently crosslinked networks that are inhomogeneous due to clusters of molecular entanglements. In chemical crosslinking, chemicals are added to create crosslinks. For PVA hydrogels, typical crosslinking agents used include glutaraldehyde, ethylaldehyde, formaldehyde, hydrochloric, boric, and maleic acid. The main drawback of using

Radial Artery Cell Seeding

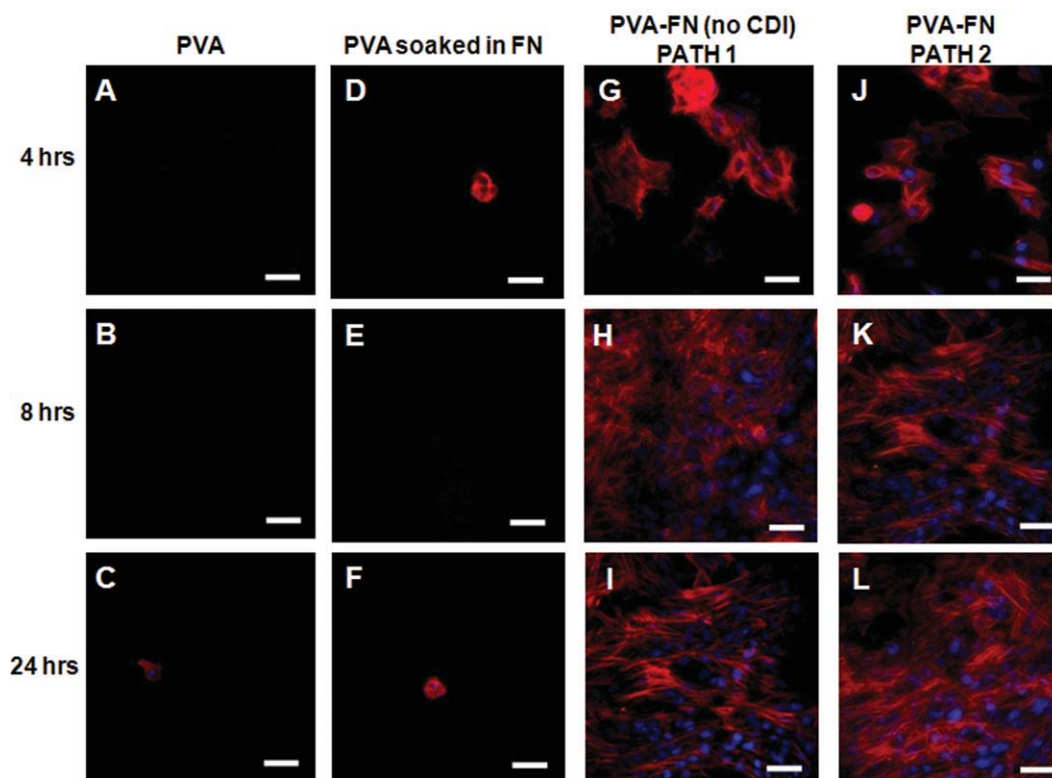


FIGURE 6. Confocal micrographs of RACs seeded onto PVA control, PVA soaked in FN, PVA-FN (without CDI), and PVA-FN (with CDI) samples. Cytoskeleton (red) was labeled with antismooth muscle α -actin (SMA)-Cy3-conjugated IgG2a primary and cell nuclei (blue) were labeled with Hoechst 33342. Note: 50 μ m scale bar. [Color figure can be viewed in the online issue, which is available at wileyonlinelibrary.com.]

chemically crosslinked PVA is that residual crosslinker will remain in the PVA matrix and eventually leach out.¹⁰ These crosslinkers are bioincompatible, making this form of PVA undesirable for *in vivo* translation.

PVA is a well-known biomaterial that has been investigated for a broad range of biomedical applications.^{10,11,15} This microstructure provides the PVA hydrogel with elastic mechanical properties similar to that displayed by several soft tissues,^{12,14,16–19,24,34} including cardiovascular tissues, making it a logical choice as the biomaterial for this study.^{16,17} Physically crosslinked PVA hydrogels are stable up to approximately 70°C. The advantage of physically crosslinked PVA is the ability to control the mechanical properties of the resulting hydrogel. Because the physiologic temperature is \sim 37°C, we and others have investigated this hydrogel material for various medical implant applications.^{10,11,15} Control of mechanical properties to mimic natural tissues, including cardiovascular tissues and cartilage, can be achieved via controlling the PVA solution concentration, number of freeze-thaw cycles, and freezing and thawing rates.^{10,16} Similar to Dacron and ePTFE, PVA is nondegradable. The ability of tuning its mechanical properties to avoid problems arising from mechanical mismatch at the anastomosis site is envisioned as an advantage over Dacron and ePTFE.

The reaction schemes for surface functionalization of PVA by FN are shown in Figure 1. Two pathways, PATH 1 and PATH 2, as shown in the figure have been investigated. The difference between these two pathways is the incorporation of an additional step using CDI in the formation of intermediate 4 in PATH 2. Our results show that both pathways lead to successful FN functionalization of the PVA surface. In the process of applying the FN functionalization reaction reported in the literature²⁰ to our physically crosslinked PVA, we discovered that it was possible to use an alternative, simpler pathway without the need of an activating step involving CDI (Figure 1). This is rather unexpected, and considering that most chemical crosslinking reactions use an excess of crosslinking agents and that physical crosslinking does not involve chemical reaction of the —OH groups in PVA, this would lead to a maximization of carboxylic acid groups in the PVA hydrogel in 3 (Figure 1). This is sufficient to drive the FN functionalization reaction leading to the direct formation of 5 (Figure 1) as evidenced by the FTIR (Figure 4) and cell seeding results (Figures 6 and 7).

The tensile mechanical properties of the PVA hydrogel before and after FN functionalization using PATH 2 are compared in Figure 2; it can be seen that there is a small stiffening effect in the PATH 2 samples compared with the PVA control. This stiffening is most likely due to the dehydrating

Endothelial Cell Seeding

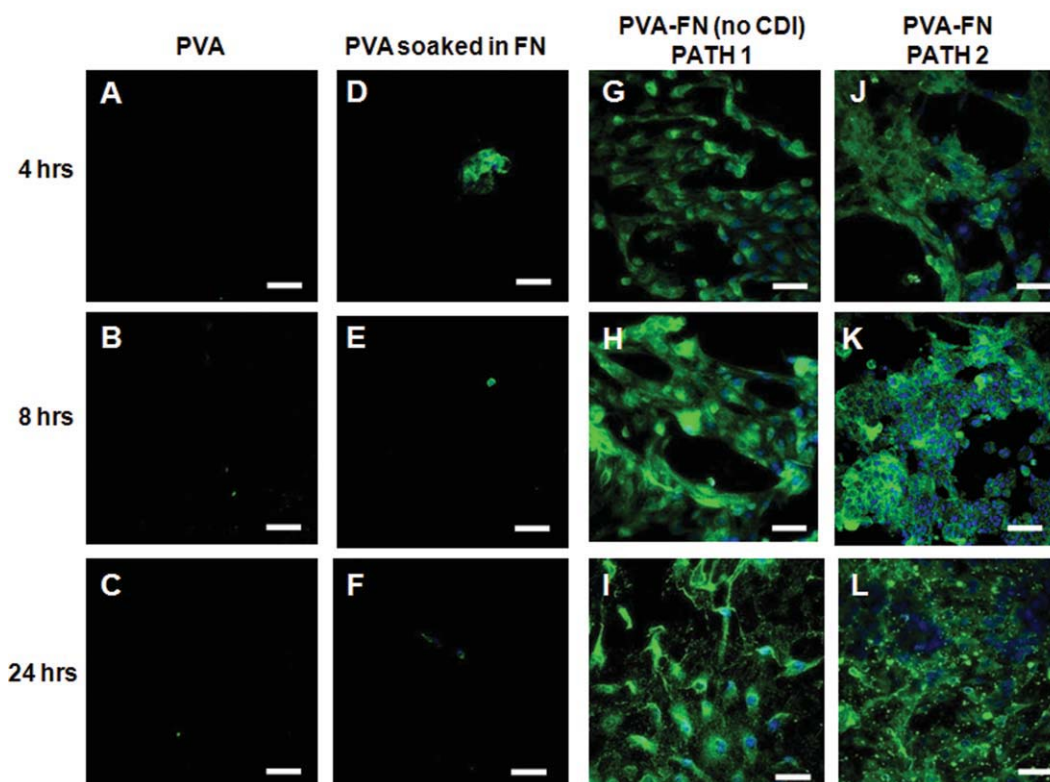


FIGURE 7. Confocal micrographs of ECs seeded onto PVA control, PVA soaked in FN, PVA-FN (without CDI), and PVA-FN (with CDI) samples. ECs were incubated with polyclonal rabbit anti-human Von Willebrand factor primary IgG and AlexaFluor[®] 488 goat anti-rabbit IgG secondary and appear green. Cell nuclei (blue) were labeled with Hoechst 33342. Note: 50 μm scale bar. [Color figure can be viewed in the online issue, which is available at wileyonlinelibrary.com.]

step required for the CDI reaction. Some of the pores in the PVA hydrogel collapse during the dehydration-rehydration process and do not reswell to the same level as before dehydration, an effect that has been reported for a similar type of PVA hydrogel.^{35,36} We have also tested the dehydration-rehydration of PVA hydrogel in distilled H_2O and observed a similar stiffening effect (data not shown). The increase in stiffness of the FN-reacted sample is therefore mainly due to the dehydration-rehydration of the PVA hydrogel and not the reaction with FN. Thus, to obtain a targeted mechanical response, the initial PVA hydrogel, before FN reaction using PATH 2, should be of a lower stiffness than desired. The elastic modulus within the physiologic range (i.e., at 30% strain) for porcine aorta in the circumferential direction is approximately 0.2 MPa.¹⁶ At this same strain, the PVA control displays a modulus of 0.32 MPa compared with 0.50 MPa for the PVA-FN samples. These values, although higher than porcine aortic tissue, are much more realistic compared with the currently available vascular graft biomaterials such as ePTFE (elastic modulus of ~ 500 MPa) and Dacron (elastic modulus of $\sim 14,000$ MPa). Both these materials have elastic moduli that are orders of magnitude larger than PVA, PVA-FN, and the intended tissues they are replacing.³

The viscoelastic response of PATH 2 samples compared with that of PVA control are shown in Figure 3. The functionalized PVA-FN relaxes at a rate comparable to the aortic tissues and the PVA control.^{16,18} Although the PVA control samples relaxed to a lower residual stress than PVA-FN, the PVA-FN values are in between the aortic tissues, indicating the ability of the functionalized PVA-FN to recover as fast as the native tissue within a cardiac cycle.

Successful FN functionalization of the PVA hydrogel is confirmed by the presence of the amide I peak at 1650 cm^{-1} in the FTIR spectra shown in Figure 4 for PATH 1 [Figure 4(B)] and PATH 2 [Figure 4(C)] samples, but not in the PVA control [Figure 4(A)]. The amide II peak at 1580 cm^{-1} is too weak to be discernable [see inset in Figure 4(C)]. Because the FTIR of product 5 is identical for both pathways, we would expect the bonding and chemical structure resulting from these pathways to be the same. Moreover, using an immunostaining method described by Nuttelman et al.,²⁰ FN fluorescence was clearly seen on both reacted samples from PATH 1 and PATH 2 at 24 hr. In contrast, unreacted PVA showed no fluorescence at 4 and 24 hr. Although some fluorescence was initially observed on the PVA samples soaked in FN solution (Figure 5), when they were placed in media, no fluorescence was observed at

4 and 24 hr (Figures 5), demonstrating that FN does not adsorb to the unreacted PVA surface. Another approach to confirm the FN functionalization reaction is via desorption using 70% isopropanol. Fluorescence of PVA-FN samples via PATHS 1 and 2 remained unchanged after the desorption step, thereby confirming that FN was covalently attached to the PVA substrate. The observation of FN fluorescence on the PATH 1 samples was rather unexpected. CDI acts to activate the —COOH end group of the side chains toward nucleophilic attack from the primary —NH_2 groups present at the N-terminus of the lysine residues of FN. Our results can be contrasted with FN functionalization of PVA reactions that require the incorporation of the CDI step (PATH 2).^{20–23} This difference may be a result of the way the PVA is crosslinked. Chemical crosslinking using reagents such as glutaraldehyde consumes a significant proportion of the —OH groups in PVA, leaving a relatively small amount of free —OH groups for reaction with 11-bromoundecanoic acid (BUDA). Thus, the lower concentration of —COOH group may require the CDI reaction to ensure effective reaction with FN. Our physically crosslinked PVA hydrogel does not suffer from —OH reduction, and its reaction with FN is effective even without the CDI activation step. Thus, our results open a faster pathway toward attachment of a protein (FN, laminin) or peptide sequences Arg-Gly-Asp (RGD) to facilitate cell attachment to a physically crosslinked PVA hydrogel with the proper mechanical properties tunable to that of soft tissues.

Cell response to the FN-functionalized PVA surfaces was assessed using two types of primary vascular cells (RACs and ECs). RACs were used to establish cell compatibility, whereas ECs would provide indication of the possibility of the formation of a nonthrombogenic surface via endothelialization. Figures 6 and 7 show cell culture results for RACs and ECs for 4 to 24 hr on the PVA control [Figure 6(A–C) and Figure 7(A–C)], PVA soaked in FN [Figure 6(D–F) and Figure 7(D–F)], PATH 1 [Figure 6(G–I) and Figure 7(G–I)], and PATH 2 [Figure 6(J–L) and Figure 7(J–L)] samples. Both type of vascular cells clearly adhered to the reacted samples (PATH 1 and PATH 2), but not to the PVA control or the PVA soaked in FN samples. RACs and ECs formed cell extensions on both reacted samples, which was a clear indication of good adhesion to the substrate. The few cells observed on the PVA control and FN-soaked PVA samples had a rounded morphology, which indicated poor adhesion to the surface, and it was expected of highly hydrophilic surfaces such as the PVA hydrogel.^{37,38} Cells used for both RACs and ECs were from known sources that have previously been phenotypically characterized.^{26,27} Cell type-specific immunostaining was performed to establish cell adhesion; thus, the aim of this procedure was not to indicate cell phenotype. PVA crosslinked using various chemical approaches has previously been investigated as a hybrid synthetic tissue³⁹ or as functionalized PVA-tissue hybrids.^{40–44} All these approaches show promising results. There have been several attempts to covalently attaching cell-adhesive proteins to PVA surface to render it more cell compatible. Schmedlen et al.²¹ reported a photocrosslinkable PVA for minimally

invasive *in situ* polymerization, which was functionalized with the cell-adhesive peptide Arg-Gly-Asp-Ser (RGDS) and found to support fibroblast attachment and spreading in a dose-dependent manner. Nuttelman et al.²⁰ reported the attachment of FN to glutaraldehyde-crosslinked PVA hydrogels, promoting 3T3 fibroblast adhesion, proliferation, and migration. This hydrogel was recommended as a possible candidate for tissue engineering scaffold. The same group later developed a photocrosslinkable, degradable PVA-poly-lactic acid copolymer with controlled degradability.⁴⁵ Zajackowski et al.²² used this same approach to show cell-matrix adhesions to the FN-functionalized hydrogel. They visualized and quantified the focal adhesions formed by human fibroblast on FN-functionalized PVA and concluded that this bioactive polymer can selectively induce specific cell-matrix adhesions important in several tissue engineering applications. Grant et al.²³ recently reported a PVA hydrogel with an adsorbed layer of hyaluronic acid and chemically crosslinked FN or laminin, using CDI activation, toward the adhesion of chondrocytes on the hydrogel surface for a tissue-engineered cartilage replacement. All these results indicate the promise of PVA-tissue hybrid as a material system for tissue replacement. Our results further demonstrate that it is possible, through a judicious choice of physically crosslinked PVA with tunable mechanical properties and a two-step FN functionalization (PATH 1), to create a PVA-FN-EC hybrid that could be hemocompatible, thus providing a first step toward an alternative for the realization of a synthetic replacement small-diameter vascular graft.

CONCLUSIONS

The PVA tissue hybrid proposed here is a biomaterial that is expected to not only behave in a manner mechanically similar to the tissue it is replacing but will also have a confluent layer of ECs that may provide the long-term nonthrombogenic characteristics required for blood-contacting applications. The successful FN functionalization of PVA without the CDI activation step was rather unexpected and is likely due to the ample availability of —OH groups in physically crosslinked PVA versus the traditional approach of chemical crosslinking. This opens up a faster and simpler pathway toward the attachment of a protein (FN, laminin) or peptide sequences (RGD) to facilitate cell attachment to a physically crosslinked PVA hydrogel with mechanical properties matching that of the tissue it is replacing. A broad range of functionalized PVA-tissue hybrid can be envisioned.

ACKNOWLEDGMENTS

The authors thank Natural Science and Engineering Research Council of Canada (NSERC) for support, NSERC and Axcelon Biopolymers Corporation for an Industrial NSERC Fellowship (Leonardo Millon), Ontario Graduate Scholarship (Donna Padavan and Amanda Hamilton), Ontario Graduate Scholarship in Science and Technology (Donna Padavan and Amanda Hamilton), and Heart and Stroke Foundation for their continuous support. The authors also thank the Canadian Institutes of Health Research Training Grant in Vascular Research (Donna Padavan and Amanda Hamilton were CIHR Training Fellows). The authors also acknowledge Dr. Kem Rogers of the

Department of Anatomy and Cell Biology for assistance and Darius Strike for EC isolation.

REFERENCES

1. Moustapha A, Anderson HV. Revascularization interventions for ischemic heart disease. *Curr Opin Cardiol* 2000;15:463–471.
2. Kannan RY, Salacinski HJ, Butler PE, Hamilton G, Seifalian AM. Current status of prosthetic bypass grafts: A review. *J Biomed Mater Res B* 2005;74B:570–581.
3. Xue L, Greisler Howard P. Biomaterials in the development and future of vascular grafts. *J Vasc Surg* 2003;37:472–480.
4. Thomas AC, Campbell JR, Campbell JH. Advances in vascular tissue engineering. *Cardiovasc Pathol* 2003;12:271–276.
5. Nerem RM, Seliktar D. Vascular tissue engineering. *Annu Rev Biomed Eng* 2001;3:225–243.
6. Rashid ST, Salacinski HJ, Fuller BJ, Hamilton G, Seifalian AM. Engineering of bypass conduits to improve patency. *Cell Prolif* 2004;37:351–366.
7. Haruguchi H, Teraoka S. Intimal hyperplasia and hemodynamic factors in arterial bypass and arteriovenous grafts: A review. *J Artif Organs* 2003;6:227–235.
8. Fung YC. *Biomechanics: Mechanical Properties of Living Tissues*. 2nd ed. New York: Springer-Verlag; 1993.
9. Hayash KSN, Meister J, Greenwald SE, Rachev A. *Techniques in the Determination of the Mechanical Properties and Constitutive Laws of Arterial Walls*. Vol.2. Boca Raton, FL: CRC Press; 2001.
10. Hassan CM, Peppas NA. Structure and applications of poly(vinyl alcohol) hydrogels produced by conventional crosslinking or by freezing/thawing methods. *Adv Polym Sci* 2000;153:37–65.
11. Lozinsky VI, Plieva FM. Poly(vinyl alcohol) cryogels employed as matrixes for cell immobilization. 3. Overview of recent research and developments. *Enzyme Microb Tech* 1998;23:227–242.
12. Kobayashi M. A study of polyvinyl alcohol-hydrogel (PVA-H) artificial meniscus in vivo. *Biomed Mater Eng* 2004;14:505–515.
13. Chu KC, Rutt BK. Polyvinyl alcohol cryogel: An ideal phantom material for MR studies of arterial flow and elasticity. *Magn Reson Med* 1997;37:314–319.
14. Wan WK, Campbell G, Zhang ZF, Hui AJ, Boughner DR. Optimizing the tensile properties of polyvinyl alcohol hydrogel for the construction of a bioprosthetic heart valve stent. *J Biomed Mater Res* 2002;63:854–861.
15. Mori Y, Tokura H, Yoshikawa M. Properties of hydrogels synthesized by freezing and thawing aqueous polyvinyl alcohol solutions and their applications. *J Mater Sci* 1997;32:491–496.
16. Millon LE, Mohammadi H, Wan WK. Anisotropic polyvinyl alcohol hydrogel for cardiovascular applications. *J Biomed Mater Res B* 2006;79:305–311.
17. Millon LE, Nieh M-P, Hutter JL, Wan W. SANS characterization of an anisotropic poly(vinyl alcohol) hydrogel with vascular applications. *Macromolecules* 2007;40:3655–3662.
18. Millon Leonardo E, Guhados G, Wan W. Anisotropic polyvinyl alcohol—Bacterial cellulose nanocomposite for biomedical applications. *J Biomed Mater Res B* 2008;86B:444–452.
19. Millon LE, Wan WK. The polyvinyl alcohol-bacterial cellulose system as a new nanocomposite for biomedical applications. *J Biomed Mater Res B* 2006;79:245–253.
20. Nuttelman CR, Mortisen DJ, Henry SM, Anseth KS. Attachment of fibronectin to poly(vinyl alcohol) hydrogels promotes NIH3T3 cell adhesion, proliferation, and migration. *J Biomed Mater Res* 2001;57:217–223.
21. Schmedlen RH, Masters KS, West JL. Photocrosslinkable polyvinyl alcohol hydrogels that can be modified with cell adhesion peptides for use in tissue engineering. *Biomaterials* 2002;23:4325–4332.
22. Zajackowski MB, Cukierman E, Galbraith CG, Yamada KM. Cell-matrix adhesions on poly(vinyl alcohol) hydrogels. *Tissue Eng* 2003;9:525–533.
23. Grant C, Twigg P, Egan A, Moody A, Smith A, Eagland D, Crowther N, Britland S. Poly(vinyl alcohol) hydrogel as a biocompatible viscoelastic mimetic for articular cartilage. *Biotechnol Prog* 2006;22:1400–1406.
24. Millon LE, Oates CJ, Wan W. Compression properties of polyvinyl alcohol—Bacterial cellulose nanocomposite. *J Biomed Mater Res B* 2009;90B:922–929.
25. Lee JM, Haberer SA, Boughner DR. The bovine pericardial xenograft. I. Effect of fixation in aldehydes without constraint on the tensile viscoelastic properties of bovine pericardium. *J Biomed Mater Res* 1989;23:457–475.
26. Johnston DE, Boughner DR, Cimini M, Rogers KA. Radial artery as an autologous cell source for valvular tissue engineering efforts. *J Biomed Mater Res A* 2006;78A:383–393.
27. Rogers KA, Boden P, Kalnins VI, Gottlieb AI. The distribution of centrosomes in endothelial cells of non-wounded and wounded aortic organ cultures. *Cell Tissue Res* 1986;243:223–227.
28. Peppas NA. Infrared spectroscopy of semicrystalline poly(vinyl alcohol) networks. *Makromol Chem* 1977;178:595–601.
29. Yang SY, Rubner MF. Micropatterning of polymer thin films with pH-Sensitive and cross-linkable hydrogen-bonded polyelectrolyte multilayers. *J Am Chem Soc* 2002;124:2100–2101.
30. Nabet A, Pea M. Two-dimensional FT-IR spectroscopy: A powerful method to study the secondary structure of proteins using H-D exchange. *Appl Spectrosc* 1997;51:466–469.
31. Rashid ST, Fuller B, Hamilton G, Seifalian AM. Tissue engineering of a hybrid bypass graft for coronary and lower limb bypass surgery. *FASEB J* 2008;22:2084–2089.
32. Ricciardi R, Mangiapia G, Lo Celso F, Paduano L, Triolo R, Auriemma F, De Rosa C, Laupretre F. Structural organization of poly(vinyl alcohol) hydrogels obtained by freezing and thawing techniques: A SANS Study. *Chem Mater* 2005;17:1183–1189.
33. Willcox PJ, Howie DW Jr, Schmidt-Rohr K, Hoagland DA, Gido SP, Pudjijanto S, Kleiner LW, Venkatraman S. Microstructure of poly(vinyl alcohol) hydrogels produced by freeze/thaw cycling. *J Polym Sci Pol Phys* 1999;37:3438–3454.
34. Stammen JA, Williams S, Ku DN, Gulberg RE. Mechanical properties of a novel PVA hydrogel in shear and unconfined compression. *Biomaterials* 2001;22:799–806.
35. Bodugoz-Senturk H, Choi J, Oral E, Kung Jean H, Macias Celia E, Braithwaite G, Muratoglu Orhun K. The effect of polyethylene glycol on the stability of pores in polyvinyl alcohol hydrogels during annealing. *Biomaterials* 2008;29:141–149.
36. Padavan DT, Hamilton AM, Millon LE, Boughner DR, Wan WK. Synthesis, characterization and in vitro cell compatibility study of a poly(amic acid) graft/cross-linked poly(vinyl alcohol) hydrogel. *Acta Biomater* 2011;7:258–267.
37. Luo Y, Shoichet MS. A photolabile hydrogel for guided three-dimensional cell growth and migration. *Nat Mater* 2004;3:249–253.
38. Wang C, Bai J, Gong Y, Zhang F, Shen J, Wang D-A. Enhancing cell affinity of nonadhesive hydrogel substrate: The role of silica hybridization. *Biotechnol Prog* 2008;24:1142–1146.
39. Cascone MG, Laus M, Ricci D, Sbarbati Del Guerra R. Evaluation of poly(vinyl alcohol) hydrogels as a component of hybrid artificial tissues. *J Mater Sci Mater M* 1995;6:71–75.
40. Lee C-T, Kung P-H, Lee Y-D. Preparation of poly(vinyl alcohol)-chondroitin sulfate hydrogel as matrices in tissue engineering. *Carbohydr Polym* 2005;61:348–354.
41. Miyashita H, Shimmura S, Kobayashi H, Taguchi T, Asano-Kato N, Uchino Y, Kato M, Shimazaki J, Tanaka J, Tsubota K. Collagen-immobilized poly(vinyl alcohol) as an artificial cornea scaffold that supports a stratified corneal epithelium. *J Biomed Mater Res B* 2006;76B:56–63.
42. Uchino Y, Shimmura S, Miyashita H, Taguchi T, Kobayashi H, Shimazaki J, Tanaka J, Tsubota K. Amniotic membrane immobilized poly(vinyl alcohol) hybrid polymer as an artificial cornea scaffold that supports a stratified and differentiated corneal epithelium. *J Biomed Mater Res B* 2007;81B:201–206.
43. Hayami T, Matsumura K, Kusunoki M, Nishikawa H, Hontsu S. Imparting cell adhesion to poly(vinyl alcohol) hydrogel by coating with hydroxyapatite thin film. *Mater Lett* 2007;61:2667–2670.
44. Mathews DT, Birney YA, Cahill PA, McGuinness GB. Vascular cell viability on polyvinyl alcohol hydrogels modified with water-soluble and -insoluble chitosan. *J Biomed Mater Res B* 2008;84B:531–540.
45. Nuttelman CR, Henry SM, Anseth KS. Synthesis and characterization of photocrosslinkable, degradable poly(vinyl alcohol)-based tissue engineering scaffolds. *Biomaterials* 2002;23:3617–3626.